Two-fluid approach for direct numerical simulation of particle-laden turbulent flows at small Stokes numbers

Babak Shotorban
Department of Mechanical and Aerospace Engineering, The University of Alabama in Huntsville, Huntsville, Alabama 35899, USA

S. Balachandar
Department of Mechanical and Aerospace Engineering, University of Florida, Gainesville, Florida 32611, USA

(Received 6 July 2008; revised manuscript received 14 February 2009; published 14 May 2009)

A two-fluid approach is proposed for direct numerical simulation of particle-laden turbulent flows in two-way coupling where the particle Stokes number is small. An Eulerian velocity field is calculated for the particle phase through a truncated series expansion in terms of the velocity and acceleration of the fluid phase [M. R. Maxey, J. Fluid Mech. **174**, 441 (1987)]. This expansion is valid for particles with a sufficiently small Stokes number defined as the ratio of particle time constant to the Kolmogorov time scale. The transport equation of the Eulerian concentration field of particles (particle volume fraction) is solved along with the fluid-phase equations for which the effect of the particles on the fluid phase is taken into account through source terms in the momentum equations. For the assessment purposes, particle-laden decaying isotropic turbulence is studied. The results obtained through the proposed two-fluid approach are compared against those obtained by the trajectory approach in which the particle equations are solved in the Lagrangian framework. It is shown that there is a good agreement between various fluid-phase statistics obtained by these approaches for different small Stokes numbers and mean particle concentrations.

DOI: 10.1103/PhysRevE.79.056703 PACS number(s): 47.11.−j, 47.55.Kf, 47.27.ek, 47.27.Gs

I. INTRODUCTION

Particle-laden turbulent flows with lots of industrial and environmental applications have been widely investigated by computational and experimental methods in the past three decades. However, a comprehensive understanding of all the relevant physical processes and of the effect of particles on turbulence structure and statistics is lacking. This is mainly due to the complexity of turbulence on one hand and the presence of additional phase of dispersed particles on the other hand. Direct numerical simulation (DNS) as a reliable and well-established tool for the study of single-phase turbulence has been widely implemented for the simulation of particle-laden turbulent flows.

The two-fluid (Eulerian-Eulerian) approach, in which the dispersed phase is considered as a second fluid with an Eulerian field representation for its properties, is an alternative to the far more highly used approach of trajectory (Eulerian-Lagrangian), in which particles are individually tracked in the Lagrangian frame, for DNS of particle-laden flows. In the two-fluid approach, the equations for the conservation of mass, momentum, and energy are obtained through an appropriate averaging process. Various averaging techniques such as time, space, and ensemble averaging have been employed in the past to develop Eulerian equations for the dispersed phase [1–5]. The main issue with the two-fluid formulation is the closure problem resulting from the averaging of particle equations. This may be one of the reasons why the DNS studies of particle-laden flows through two-fluid approaches are scarce for the case of a turbulent carrier-phase turbulent flow. Druzhinin and Elghobashi [6] studied a decaying isotropic turbulence laden with particles of small Stokes number, which is a nondimensional number defined as the ratio of the particle time scale and the turbulence Kolmogorov time scale, in the two-way coupled regime. Proposing a two-fluid model named as the mesoscopic Eulerian approach, Fevrier *et al.* [7] and Kaufmann *et al.* [8] studied isotropic turbulence in the context of flows in one-way coupling. Rani and Balachandar [9] and Shotorban and Balachandar [10] studied the forced isotropic and homogeneous shear turbulence using the equilibrium Eulerian two-fluid approach. Most recently, Boffetta *et al.* [11] studied the regularity and compressibility of the particle velocity field in two-dimensional (2D) and three-dimensional (3D) isotropic turbulent flows through the two-fluid approach.

A robust two-fluid formulation can be readily developed for particles with a sufficiently small Stokes number. In this formulation, the particle Eulerian velocity is approximately expressed in terms of the surrounding fluid-phase velocity and its temporal and spatial derivatives through a series expansion [12–15]. This two-fluid approach is called equilibrium Eulerian approach [14] which is tested in isotropic and homogeneous shear turbulent flows in one-way coupling [9,10] by comparing its results against the results obtained by the trajectory approach. The main advantage of the equilibrium Eulerian approach is that the Eulerian velocities of the dispersed phase can be explicitly computed from the velocities of the carrier phase and no differential equations are required to solve for the momentum equation of the dispersed phase. On the other hand, the disadvantage is that it is only applicable to particles with small Stokes numbers. Two major applications of the equilibrium Eulerian model have been in the simulation of aluminum-oxide smoke particles in the solid rocket motors [16] and gravity currents driven by inertial particles [17]. This model has been recently extended to large-eddy simulation (LES) [18]. It should be also mentioned here that the series expansion used in the development of the equilibrium Eulerian approach has been the base of the

theoretical studies on the intermittent particle distribution in turbulent flows [19–22]. Recent high-resolution DNS study of particle-laden isotropic turbulence by Bec *et al.* [23] through trajectory approach shows that the particle acceleration well approximated by the carrier-phase acceleration for particles with small Stokes numbers. This approximation is equivalent to the series-expansion approximation for the particle velocity in the equilibrium Eulerian approach.

In the present work, we extend our previous studies on the equilibrium Eulerian approach for the DNS of particle-laden turbulent flows from one-way coupling to two-way coupling. In the following sections, first, we present the equilibrium Eulerian formulation for two-way coupling and then we employ it for the DNS of a decaying isotropic turbulent flow. The results obtained by this approach are compared against those obtained by the trajectory approach for assessment purposes.

II. MATHEMATICAL FORMULATION

In the two-phase particle-laden flow considered in this study, the fluid phase is an incompressible Newtonian fluid and the particle phase is composed of a large number of monodispersed spherical particles of diameter much smaller than the smallest length scale of the fluid-phase flow. The governing equations of the particle position and velocity in the Lagrangian frame are

$$\frac{dx_{pi}}{dt} = V_i, \tag{1}$$

$$\frac{dV_i}{dt} = \frac{1}{\tau_p}(U_i - V_i), \tag{2}$$

where x_{pi} and V_i are the particle instantaneous position and velocity, respectively. U_i is the velocity of the carrier phase at the location of the particle. $\tau_p = \mathrm{Re}_0\ \gamma d_p^2/18$ represents the particle time constant where Re_0 is the reference Reynolds number, d_p is the nondimensional diameter of the particle, and $\gamma = \rho_p/\rho$ is the density ratio of the particle to fluid phase. In general additional forces such as pressure gradient, added mass, buoyancy, and Basset history forces must be included on the right-hand side of the particle momentum equation; however, for a high ratio of particle and fluid density, e.g., $\gamma = 1000$ considered in this study, these forces can be neglected [24]. This neglect has been justified by Armenio and Fiorotto [25] for a turbulent channel flow.

Provided that $\mathrm{St} \ll 1$ where $\mathrm{St} = \tau_p/\tau_\eta$ is the Stokes number with τ_η representing the Kolmogorov time scale, the velocity of the particle can be approximated as

$$V_i = U_i - \tau_p \frac{DU_i}{Dt}, \tag{3}$$

where DU_i/Dt is the acceleration of the fluid phase. Calculated by this equation, V_i is called the equilibrium Eulerian velocity [10,14,26] which can be used to solve the transport equation of particle concentration (volume fraction),

$$\frac{\partial \Phi}{\partial t} + \frac{\partial (\Phi V_i)}{\partial x_i} = 0. \tag{4}$$

Equation (3) was obtained for the first time by Maxey [12] through a series expansion for the velocity of the particle in Eq. (2). This equation is of the first-order accuracy with respect to τ_p. Higher-order approximations were also derived later by Druzhinin [13], Ferry and Balachandar [14], Ferry *et al.* [26], and Dodin and Elperin [15].

It is clear that with the increase in the Stokes number the accuracy of the equilibrium Eulerian will decrease because the contribution of the truncated terms of the second and higher powers of τ_p on the right-hand side of Eq. (3) will increase. Thus the equilibrium Eulerian method will be more of use if one can have an idea on its validity for the Stokes numbers considered. In other words one will need to know roughly the Stokes number above which the approximation made for the particle velocity via Eq. (3) is not reasonable. As we have done in our previous studies in the case of one-way coupling [9,10] and in the case of two-way coupling in the current study, a rigorous test is to conduct Lagrangian particle simulation for various Stokes numbers and compare the Lagrangian results versus the results predicted by the equilibrium Eulerian. This methodology is precise in quantifying the performance of equilibrium Eulerian approach for various Stokes numbers. However, in the practical applications one should be able to evaluate the accuracy of the equilibrium Eulerian model used for the considered Stokes number without conducting Lagrangian simulations. One way to do so is to include the term of τ_p^2 in the series-expansion equation, i.e., Eq. (3) and compute a second-order equilibrium Eulerian velocity

$$V_i = U_i - \tau_p \frac{DU_i}{Dt} + \tau_p^2 \left(\frac{D^2 U_i}{Dt^2} + \frac{DU_j}{Dt} \frac{\partial U_i}{\partial x_j} \right). \tag{5}$$

The derivation of this equation can be found in [13–15]. We refer to the V_i computed by Eq. (5) as the second-order equilibrium Eulerian velocity while we refer to that computed by Eq. (3) as the first-order equilibrium Eulerian velocity. Comparing the magnitude of the first- and second-order equilibrium Eulerian velocities will give an idea on how much the contribution of the truncation error is.

The common practice for the DNS of particle-laden flows in two-way coupling for a dilute concentration of particles, e.g., $\langle \Phi \rangle < O(10^{-3})$, and a high ratio of particle density to the carrier-phase density, e.g., $\gamma = 1000$, is to account for the effect of particles on the carrier phase by adding a source term to the equations of the carrier phase and neglecting the variation in Φ on the continuity equations and the rest of the terms in the momentum equation of the carrier phase [27–29]. Therefore, the continuity and momentum equations of the carrier phase read

$$\frac{\partial U_i}{\partial x_i} = 0, \tag{6}$$

TABLE I. The carrier-phase properties of turbulence at $t=0$.

Re_λ	U_{rms}	$\eta\kappa_{\max}$	τ_η	u_η
56.24	0.4082	1.112	0.1717	0.1628

$$\frac{DU_i}{Dt} = -\frac{\partial P}{\partial x_i} + \frac{1}{\mathrm{Re}_0}\frac{\partial^2 U_i}{\partial x_j \partial x_j} - \mathcal{S}_i, \tag{7}$$

where $DU_i/Dt = \partial U_i/\partial t + U_j \partial U_i/\partial x_j$. In Eq. (7), $\mathcal{S}_i$ is the source term taking into account the effect of two-way coupling. This term in the Lagrangian approach is calculated by

$$\mathcal{S}_i = \gamma \frac{n_{\mathrm{p}} V_{\mathrm{p}}}{V_{\mathrm{cell}}} \sum_{k=1}^{N_{\mathrm{cell}}} F_{ik}, \tag{8}$$

where n_{p} is the number of particles that each computational particle represents, N_{cell} is the number of computational particles in the cell, V_{cell} is the volume of the computational cell, and $F_{ik} = (U_i^k - U_{\mathrm{p}i}^k)/\tau_{\mathrm{p}}$. Equation (8) is the source term equation used in [28,30,31] which is modified here to account for computational particles. It is noted that in the DNS of particle-laden turbulence, the number of actual particles may be so large that the tracking of each particle is not computationally possible, in which case, only a small number of particles are tracked and each of these particles, which is referred to as a computational particle, represents a definite number of actual particles. In the two-fluid approach,

$$\mathcal{S}_i = \frac{\gamma}{\tau_{\mathrm{p}}}\Phi(U_i - V_i), \tag{9}$$

where V_i and Φ are obtained from Eqs. (3) and (4), respectively, in the equilibrium Eulerian formulation. The source term in Eq. (9) is the same used by L'vov *et al.* [32] and Hogan and Cuzzi [33].

Here we would like to mention that the pressure-correlated dispersion of particles recently studied by Luo *et al.* [34] can be readily shown for incompressible flows and small Stokes numbers by equilibrium Eulerian approximation in one-way coupling. The divergence of the momentum equation for an incompressible carrier phase results in $\partial_i(DU_i/Dt) = -\partial_i\partial_i P$ where P denotes pressure divided by the density of the fluid and $\partial_i(\,) \equiv \partial(\,)/\partial x_i$. Also, performing the divergence operation on Eq. (3) and substituting for $\partial_i(DU_i/Dt)$, one can derive $\partial_i V_i = \tau_{\mathrm{p}}\partial_i\partial_i P$ which shows the obvious correlation between the Laplacian of the carrier-phase pressure and the compressibility of the dispersed-phase velocity field.

III. OVERVIEW OF SIMULATIONS

In order to assess the equilibrium Eulerian formulation in two-way coupling, a particle-laden decaying isotropic turbulent flow is studied. In this configuration, the initial velocity is generated by random numbers with the Passot-Pouquet [35] energy spectrum $E(\kappa) \propto \kappa^4 \exp(-2\kappa^2/\kappa_{\mathrm{m}}^2)$ with $\kappa_{\mathrm{m}}=7$. This velocity field also satisfies the continuity equation. Table I shows turbulence parameters of the initial velocity field. All DNS simulations are performed on a 128^3-node mesh with a domain dimension of $(2\pi)^3$. This number of nodes is sufficient for the considered Re_λ since the condition of $\eta\kappa_{\max} > 1$ with $\kappa_{\max}$ denoting the maximum resolved wave number is satisfied at all times. All Eulerian equations are solved using a pseudospectral method [36]. The momentum coupling term is set to $\mathcal{S}_i=0$ in Eq. (7) until the "injection time." This is the time when particles with a uniform distribution are released in the Lagrangian approach through turning on the coupling term in Eq. (7). In the equilibrium Eulerian approach, the Eulerian particles are released with $\Phi/\langle\Phi\rangle = 1$ at the injection time. The injection time is set to $t_{\mathrm{inj}}=0.8$ in all Lagrangian and equilibrium Eulerian simulations. Also, the initial velocities of particles are set equal to their local fluid-phase velocities. The number of computational particles tracked is $N_{\mathrm{p}}=128^3$ in all Lagrangian simulations. It is noted that to study the effect of two-way coupling in the Lagrangian approach, one computational particle per cell will generate fluid-phase results independent from the total number of computational particles reasonably well when $\langle\Phi\rangle$ is small of $\mathcal{O}(10^{-3})$ [27] (the largest $\langle\Phi\rangle = 0.4 \times 10^{-3}$ in the present work). Cases with various particle parameters studied in this work are displayed in Table II. In all these cases $\rho_{\mathrm{p}}/\rho = 1000$. On a system with an AMD Opteron 1212 Dual Core 2.0 GHz CPU and 2 Gbit memory, it takes 675 min to complete an equilibrium simulation while it takes 875 min to complete a Lagrangian simulation.

TABLE II. Dispersed-phase properties in different cases.

Case	τ_{p}	St[a]	$\langle\Phi\rangle$
A	0.02678	0.1	one way
B	0.02678	0.1	0.2×10^{-3}
C	0.02678	0.1	0.4×10^{-3}
D	0.06695	0.25	0.2×10^{-3}

[a] $\mathrm{St} = \tau_{\mathrm{p}}/\tau_\eta$ where τ_η is given at the injection time $t=0.8$.

IV. RESULTS

To evaluate the accuracy of the equilibrium Eulerian formulation, we first conduct *a priori* test in which we compare first- and second-order equilibrium approximations for particle velocities calculated by Eqs. (3) and (5), respectively. The purpose of this test is to quantitatively assess the contribution of the truncation error involved in approximating the particle velocity in terms of the powers of τ_{p}, and fluid velocity and its high-order derivatives. As follow, we describe how the *a priori* test is carried out in the present work. Similar tests may be carried out for configurations other than isotropic turbulence if one wishes to assess the equilibrium Eulerian model.

Seen in Fig. 1 are the root mean squares (rms) of fluid and equilibrium Eulerian velocities and their ratio in one-way coupling. The rms is defined as $U_{1,\mathrm{rms}} = \sqrt{\langle U_1^2\rangle}$ and $V_{1,\mathrm{rms}} = \sqrt{\langle V_1^2\rangle}$ for the fluid and equilibrium Eulerian velocities, respectively, and the first- and second-order $V_{1,\mathrm{rms}}$ are calculated via Eqs. (3) and (5), respectively. In the decaying iso-

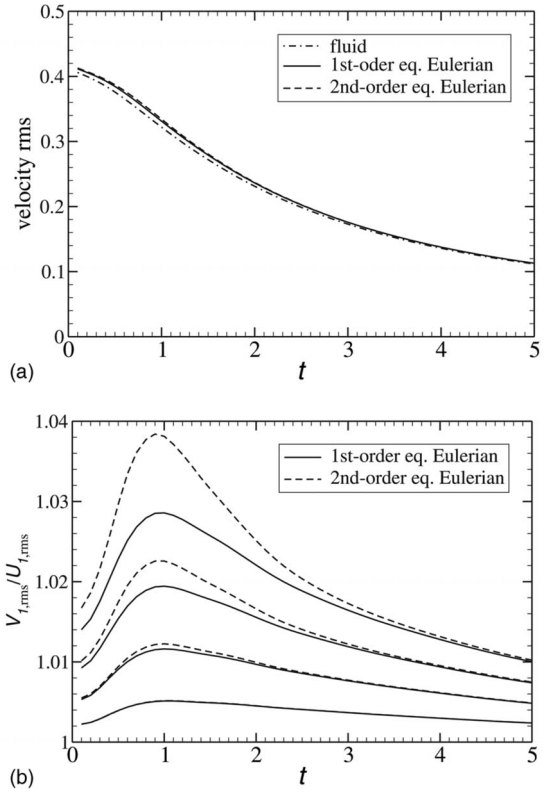

FIG. 1. (a) Time evolution of the root mean squares of fluid and equilibrium Eulerian velocities for Stokes number St=0.2; (b) time evolution of the ratio of the equilibrium Eulerian velocity to the fluid velocity for St=0.1, 0.2, 0.3, and 0.4 in increasing order from the bottom to the top curves.

tropic turbulence the lack of any turbulence production results in the so-called decay of turbulence as seen in Fig. 1(a), $U_{1,\mathrm{rms}}$ decreases in time. Using the homogeneity property of the isotropic turbulence, it could be shown through Eq. (3) that

$$\langle V_1^2\rangle = \langle U_1^2\rangle + \tau_p^2\left\langle\left(\frac{DU_1}{Dt}\right)^2\right\rangle - \tau_p\frac{\partial\langle U_1^2\rangle}{\partial t}. \tag{10}$$

Two last terms on the right-hand side of this equation are positive. The positivity of the last term is due to the negative rate of change in $U_{1,\mathrm{rms}}$ as observed in Fig. 1(a). Thus the observation made for $U_{1,\mathrm{rms}}$ being smaller than $V_{1,\mathrm{rms}}$ at all times in Fig. 1(a) is justified. The difference between first- and second Eulerian velocity root mean squares which is calculated at St=0.2 is not much distinguishable in Fig. 1(a), so to better observe their difference, they are nondimensionalized by $U_{1,\mathrm{rms}}$ and displayed in Fig. 1(b). This nondimensionalized quantity is calculated and shown for four different Stokes numbers ranging from 0.1 to 0.4 with 0.1 increments. The nondimensionalization better shows the difference between first- and second-order equilibrium Eulerian velocities. This difference with a maximum at around $t=1$ is the most significant for St=0.4 among all shown Stokes numbers. This is due to the fact that the third term on the right-hand side of Eq. (5), which is truncated in Eq. (3), makes more

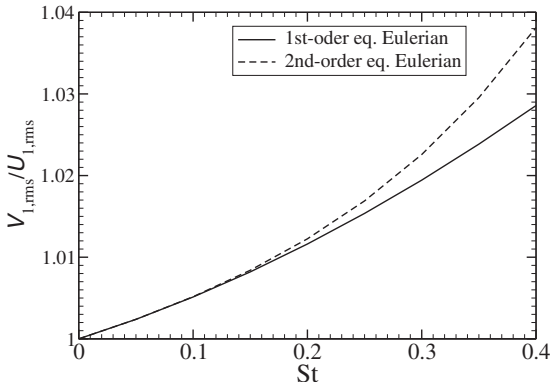

FIG. 2. The ratio of root mean squares of fluid and equilibrium Eulerian velocities versus Stokes number at time $t=1$.

contribution with the increase in the Stokes number.

Figure 2 presents the variation in $V_{1,\mathrm{rms}}/U_{1,\mathrm{rms}}$ against Stokes number at $t=1$ around which time the maximum difference between the first- and second-order equilibrium Eulerian velocities occurs as observed in Fig. 1(b). In Fig. 2, it is seen that up to St=0.1 the curves of the first-order and second-order equilibrium Eulerian velocities are on top of each other and their difference is not recognizable in the figure. A relative error defined by $e=|V_{1,\mathrm{rms}}^{(1)}-V_{1,\mathrm{rms}}^{(2)}|/|V_{1,\mathrm{rms}}^{(1)}-U_{1,\mathrm{rms}}|$ where superscripts (1) and (2) denote the first- and second-order equilibrium approximations, respectively, better displays their difference and so the magnitude of the truncation error associated with the first-order equilibrium Eulerian approximation is quantified. This relative error is calculated as $e=5\%$, 9%, and %16 for Stokes numbers 0.2, 0.25, and 0.3, respectively. Having carried out such estimation of error associated with the equilibrium Eulerian approximation in one-way coupling, we restrict our simulations to Stokes numbers below 0.25 and perform more rigorous tests of equilibrium Eulerian method by comparing the statistics predicted by it to those obtained through Lagrangian simulations of particles. These tests are referred as *a posteriori* tests.

Figure 3 shows the time evolution of mean turbulent kinetic energy $k=\langle U_iU_i\rangle/2$ in the considered decaying isotropic turbulence in one-way coupling and two-way coupling

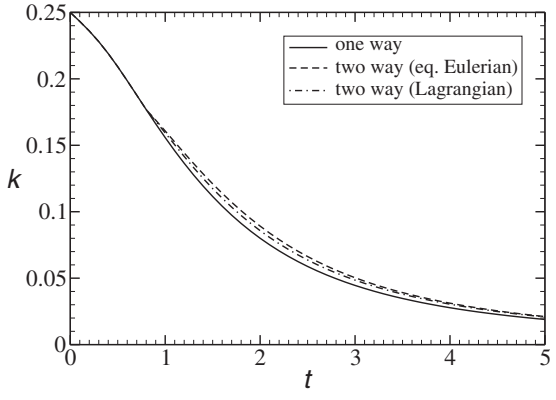

FIG. 3. Time evolution of the mean turbulent kinetic energy in one- and two-way couplings for St=0.1; $\langle\Phi\rangle=0.4\times10^{-3}$ in two-way coupling.

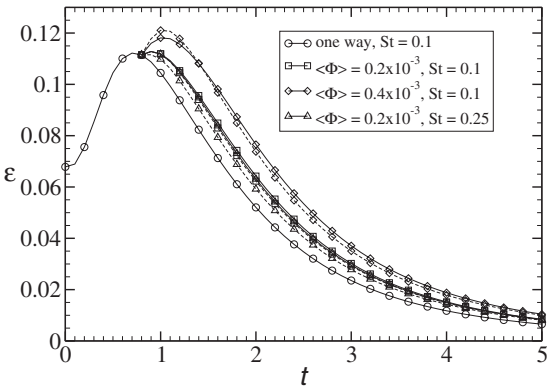

FIG. 4. Time evolution of the dissipation rate of the mean turbulent kinetic energy in equilibrium Eulerian (solid line) and Lagrangian (dashed line).

for St=0.1. As seen in this figure, the mean turbulent kinetic energy cannot maintain in the decaying isotropic turbulence. It decreases as time progresses because turbulence is not produced in the absence of random forcing term or mean velocity gradient. It is observed in this figure that at all times k is larger in the cases of two-way coupling than that in the case of one-way coupling. Through Lagrangian DNS, a similar observation was made by Ferrante and Elghobashi [29] for small Stokes numbers. It can be seen in Fig. 3 that k is slightly smaller in the Lagrangian two-way case than that in the equilibrium Eulerian one. To understand the mechanism of modification of the turbulent kinetic energy by particles with small Stokes numbers, we study the so-called budget equation of the mean turbulent kinetic energy. This equation in the decaying isotropic turbulence reads

$$\frac{dk}{dt} = -\varepsilon + \varepsilon_p, \tag{11}$$

where $\varepsilon = 2\langle S_{ij}S_{ij}\rangle/\mathrm{Re}_0$ with $S_{ij}=(\partial U_i/\partial x_j + \partial U_j/\partial x_i)/2$ as the dissipation rate. In Eq. (11) $\varepsilon_p = -2\langle U_i \mathcal{S}_i\rangle$ where $\mathcal{S}_i$ calculated by Eqs. (8) and (9) in the Lagrangian and equilibrium Eulerian approaches, respectively, is the rate of change in the mean turbulent kinetic energy due to the coupling term in Eq. (7).

Shown in Fig. 4 is the temporal variation in the dissipation rate of the mean turbulent kinetic energy. This quantity is the same for all cases until the injection time $t=0.8$ before which there is no particle back-way coupling effect on the fluid because during this time the coupling term is turned off. After particles are injected, ε in two-way coupling cases starts deviating from that in the one-way coupling case. It reaches a maximum value at around $t=1$ in two-way coupling cases. The decay rate of the mean turbulent kinetic energy, i.e., dk/dt, is attributed to ε as well as ε_p in two-way coupling according to Eq. (11). k for the case of two-way coupling is slightly larger than that for the one-way coupling as seen in Fig. 3. Thus, it would be reasonable here to assume that dk/dt is almost the same for both one- and two-way coupling cases at the studied Stokes number. On the other hand, ε is significantly larger for two-way coupling cases as seen in Fig. 4. So it could be concluded that ε_p is a positive value in two-way coupling cases according to Eq. (11). This means that ε_p is a production term in this equation for the mean turbulent kinetic energy at small Stokes numbers. The physical mechanism of modification of turbulence in two-way coupling for particles with small Stokes numbers is well explained by Ferrante and Elghobashi [29]. The trajectory of particles with small particle time constants is almost identical to the trajectory of the fluid particles while their kinetic energy is larger because their density is larger than that of the surrounding fluid. Therefore, $\langle U_i V_i\rangle$ is larger than $\langle U_i U_i\rangle$ and as a result according to the definition of $\varepsilon_p = 2\langle U_i \mathcal{S}_i\rangle$ with $\mathcal{S}_i$ calculated by Eq. (9), ε_p has a positive value. It is also seen in Fig. 4 that there is a good agreement between the Lagrangian and equilibrium Eulerian cases on ε in two-way coupling. However, in all these cases, excluding a short period of time right after injection for the case with $\langle\Phi\rangle = 0.2\times 10^{-3}$ and St=0.25, the Lagrangian results are slightly overpredicted by the equilibrium Eulerian results at all times. In the case with St=0.25, this overprediction is more pronounced.

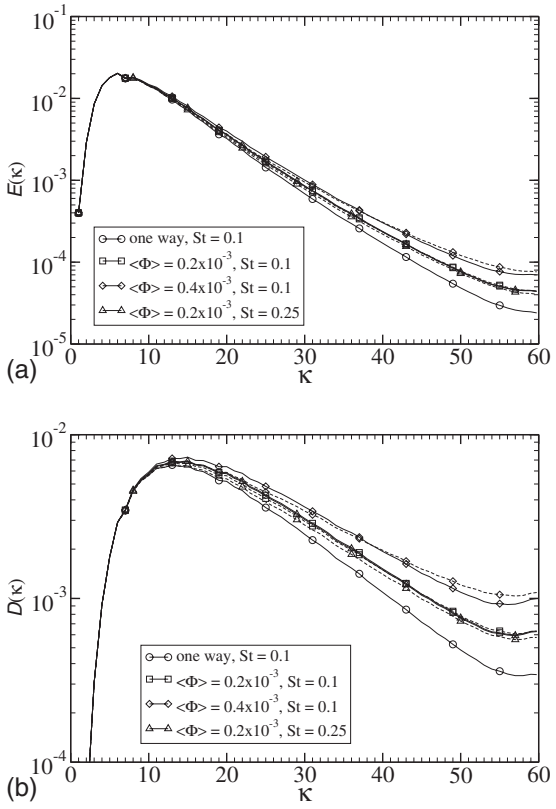

FIG. 5. (a) Spectra of turbulent kinetic energy; and (b) spectra of the dissipation rate of turbulent kinetic energy at $t=1.5$ in equilibrium Eulerian (solid line) and Lagrangian (dashed line).

Shown in Fig. 5(a) are the spectra of the turbulent kinetic energy $E(\kappa)$ and the dissipation rate $D(\kappa)$, respectively. As can be seen, $E(\kappa)$ and $D(\kappa)$ are larger at high wave numbers in two-way coupling compared to those in one-way coupling. The back-way coupling effect of particles with small stokes numbers as stated earlier is to increase the turbulent kinetic energy. Furthermore, particles at small Stokes numbers, which have small particle time constants, mainly interact with small scales of turbulence. Thus, the production of en-

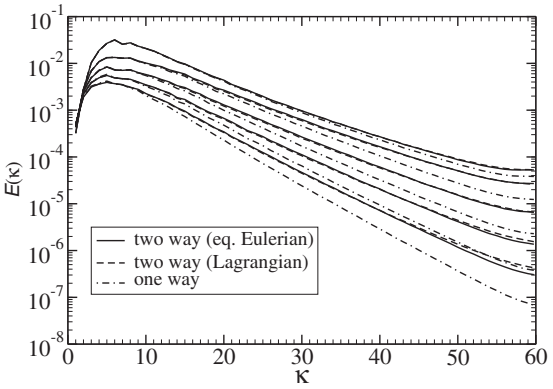

FIG. 6. Energy spectra for St=0.1 and $\langle\Phi\rangle=0.2\times10^{-3}$ at various times $t=1$, 2, 3, 4, and 5 from the top to the bottom.

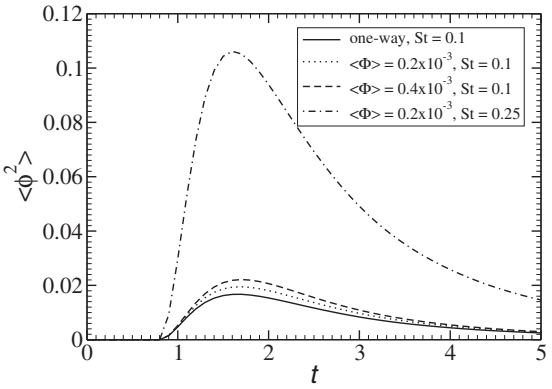

FIG. 7. Evolution of nondimensional variance of particle concentration in equilibrium Eulerian.

ergy due to the motion of small Stokes-number particles primarily takes place at small scales of turbulence. This is the reason for a larger $E(\kappa)$ in two-way coupling at high wave numbers as observed in Fig. 5(a). It is noted that a part of energy produced by the motion of particles dissipates due to the viscosity. Thus, the increase in the dissipation rate spectra at high wave numbers seen in Fig. 5(b) could be attributed to this. It seems that in Fig. 5 all scales of turbulence, excluding $\kappa<10$ are modified in two-way coupling. However, we notice that our DNS is carried out at low Reynolds number and we do not have a broad inertial subrange. Whether at high Reynolds turbulence with a broad range of inertial subrange, particles with small Stokes numbers will be able to modify a wide range of scales is an open question. In fact, to verify Kolmogorov's $-5/3$ power law for the case of two-way coupling with small Stokes-number particles, large-scale computations that can generate a broad inertial subrange will be required. Seen in Fig. 5 is also the increase in $\langle\Phi\rangle$ that results in a more pronounced increase in $E(\kappa)$ and $D(\kappa)$. A similar observation has been made by Ferrante and Elghobashi [29] for $E(\kappa)$. In Fig. 5(a), a good match between the Lagrangian and equilibrium Eulerian simulations is seen for $E(\kappa)$ in all two-way coupling cases. In the case with $\langle\Phi\rangle=0.4\times10^{-3}$ and St=0.1, $E(\kappa)$ obtained from the Lagrangian approach is slightly underpredicted by the equilibrium Eulerian approach at $\kappa>40$. On the other hand, at the same $\langle\Phi\rangle$ and larger St=0.25, it is overpredicted by the equilibrium Eulerian approach. This overprediction is more pronounced for $D(\kappa)$ as seen in Fig. 5(b). The increase in deviation between the Lagrangian and equilibrium Eulerian spectra for the case with a larger Stokes number can be attributed to a larger truncation error in the equilibrium Eulerian approximation. As shown in Fig. 2 this error is larger for St=0.25 compared to St=0.1. On the other hand, a larger discrepancy between equilibrium Eulerian and Lagrangian, observed in Fig. 5 for the case with larger $\langle\Phi\rangle$, could be attributed to the computational particles which must represent a larger number of real particles in this case.

Figure 6 shows the turbulent kinetic-energy spectra at various times. The energy spectra decrease at all wave numbers as time progresses. This is consistent with the observation made in Fig. 3 as the mean turbulent kinetic energy $k\equiv\int E(\kappa)d\kappa$ decreases with the increase in time. In the particle-laden isotropic turbulence, the rate of change in energy spectra is due to the spectral energy-transfer rate or triadic interaction of wave numbers [37], which is responsible for the interaction of various scales of turbulence, the dissipation rate spectra, which is responsible for the energy dissipation, and the two-way coupling term energy spectra, which is responsible for the direct particle-turbulence interaction [29]. Right after injection, particles start modifying the energy spectra at high wave numbers because at small Stokes numbers particles more directly interact with the small scales of turbulence. As seen in Fig. 6, at $t=1$, which is very close to the injection time, the energy spectra in two-way coupling cases is larger than that in one-way coupling mainly at $\kappa>20$. The energy spectra in two-way coupling remain larger as time progresses. With the increase in time it is seen that the wave number beyond which the deviation between one-way and two-way couplings becomes visible shifts toward smaller wave numbers. This wave number is around $\kappa=20$ and $\kappa=10$ at $t=1$ and $t=5$, respectively. The agreement between the Lagrangian and equilibrium Eulerian approaches is very good at all times. However, at large wave numbers of $\kappa>40$, $E(\kappa)$ is slightly larger for Lagrangian cases compared to their equilibrium Eulerian counterparts at later times.

Figure 7 presents the time advancement of the nondimensional variance of particle concentration $\langle\phi^2\rangle\equiv\langle(\Phi-\langle\Phi\rangle)^2\rangle/\langle\Phi\rangle^2$. The variance of particle concentration can indicate how much particles are accumulated or so-called clustered. Particle accumulation phenomenon is briefly described here. As particles move in the flow, they avoid turbulence vorticity cores due to their inertia interaction with turbulent vortices which results in centrifugal forces that expel particles from high vorticity-magnitude regions. Thus a less number of particles are found in these regions. With the increase in the Stokes number, more accumulation is seen for particles since high Stokes-number particles possess higher inertia and therefore, experience stronger centrifugal forces. However, there is a critical Stokes number after which its increase results in less accumulation of particles. In a recent one-way coupled DNS study, Bec *et al.* [38] obtained the critical Stokes number $\mathrm{St}\approx0.6$ for Lagrangian particles in forced isotropic turbulence and showed that its value unchanged with the change in Re_λ. For Stokes numbers larger

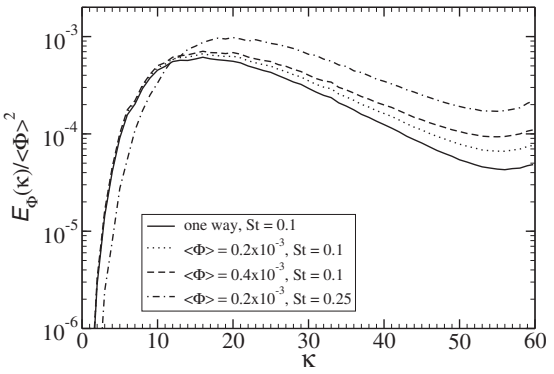

FIG. 8. Energy spectra of particle concentration in equilibrium Eulerian at $t=2$.

than the critical value, the inertia of particles is so high that small vortices are not strong and effective to influence the trajectory of individual particles as much as they are for particles with small Stokes numbers. These particles primarily interact with larger vortices so they still cluster but not as much as particles with critical Stokes numbers do. Very large Stokes-number particles move much more chaotically and independently from the surrounding fluid motions. Such particles will be found more uniformly distributed in the domain of the homogeneous turbulent flow if they are uniformly distributed at the injection time. All Stokes numbers studied in the present work are below the critical value so we expect to see the increase in particle clustering with the increase in the Stokes number. For all cases displayed in Fig. 7 the particle concentration variance starts growing from the zero value at the injection time $t=0.8$. Then, it reaches a maximum value at around $t=1.6$. After this maximum point, $\langle\phi^2\rangle$ monotonically decreases until the end of the simulation. Uniformly distributed particles at $t=0$ with zero concentration variance migrate to regions of low vorticity due to particle clustering phenomena so the concentration variance increases after injection. In fact, this migration time is the initial period where the particle concentration variance rapidly grows from zero as could be seen in Fig. 7. On the other hand, after a short while the time-dependent Stokes number of particles defined by $\mathrm{St}(t)\equiv\tau_p/\tau_\eta(t)=\tau_p\,\mathrm{Re}^{1/2}\,\varepsilon(t)^{1/2}$, where $\varepsilon(t)$ denotes the dissipation rate at time t, decreases since as seen in Fig. 4, $\varepsilon(t)$ decreases after $t=1$. In reality it is the time-dependent Stokes number which dictates the particles on how much to accumulate. The time-dependent Stokes number decreases with time after $t=1$ since $\varepsilon(t)$ decreases after this time. This is the reason for less accumulation of particles and the decrease in particle concentration variance after around $t=1.5$. As displayed in Fig. 7, the variance of particles is the largest for the case with St=0.25 at all times which is because of the larger accumulation of particles for larger Stokes numbers. With the increase in $\langle\Phi\rangle$ while keeping the Stokes number constant St=0.1, the variance of particle increases. This is attributed to the fact that the time-dependent Stokes number increases with the increase in $\langle\Phi\rangle$ since the dissipation rate ε seen in Fig. 4 is larger for larger $\langle\Phi\rangle$.

In Fig. 8, the energy spectra of particle concentration normalized by the mean concentration are shown for various cases at $t=2$. This quantity represents the contribution of each scale to the variance of particle concentration. Comparing this figure to Fig. 5 of turbulent kinetic-energy spectra shows that unlike turbulent kinetic energy, small scales significantly contribute to the variance of particle concentration. This implies the existence of sharp gradients of particle concentration at small scales where the velocity field is much smoother. This is also an indication of preferential concentration of particles at small scales. Such preferential concentration may not be found in large scales as in wave numbers below around $\kappa<10$ for St=10 and $\kappa<14$ for St=0.25, the energy spectra of particle concentration sharply decrease with the decrease in wave numbers. It could be seen in Fig. 8 that at constant Stokes number St=0.1, $E_\Phi(\kappa)/\langle\Phi\rangle^2$ is almost the same at small wave numbers in one- and two-way coupling cases. Starting from $\kappa>10$ for St=0.1, the particle concentration energy spectra become larger for two-way coupling cases. So the increase in particle concentration variance with the increase in $\langle\Phi\rangle$ as observed in Fig. 7 is mainly because of the energy spectra of particle concentration at $\kappa>10$.

We should add here that it would be ideal to compare the variance and energy spectra of particle concentration obtained by the equilibrium Eulerian, as shown in Figs. 7 and 8, versus those obtained by the Lagrangian approach. To do so, one will need to have a large number of particles (computational particles) in each computational cell that generates sufficient statistical samples. In other words, Lagrangian particles need to be coarse grained on η^3-size bins (the Kolmogorov scale η is approximately equal to the computational cell size in DNS) as there are clusters (voids) of size comparable to the Kolmogorov scale at small Stokes numbers [38]. In a recent study carried out by Kaufmann *et al.* [8], 80 computational particles per cell was used in the Lagrangian simulations to compare the particle concentration statistics to those obtained by the Eulerian simulations. This number of particles is 80 times larger than the number of particles (computational particles) used in the present study where Lagrangian computations are performed, implementing one particle per cell as mentioned in Sec. III. So we would need 80×128^3 particles in all computational domain (80 times more computational particles) if we wanted to calculate the concentration variance and spectra via the Lagrangian approach. Such a large number of particles are not feasible to carry out the computation for using our code and computational resources.

V. CONCLUDING REMARKS

For direct numerical simulation of particle-laden turbulent flows in two-way coupling, a two-fluid approach is proposed in which particles are also dealt with in the Eulerian framework. The main assumption made in this approach, which is named as the equilibrium Eulerian approach, is that the velocity of the particle phase can be expressed in terms of the velocity and acceleration of the fluid phase [12]. This assumption is only valid for particles with sufficiently small Stokes numbers; however, there is an advantage of not solving any partial differential equations for the particle-phase Eulerian velocity field. The equilibrium Eulerian formulation

is implemented to simulate a particle-laden decaying isotropic turbulent flow, and *a priori* and *a posteriori* tests are carried out for it. In the *a priori* test, the first- and second-order Equilibrium Eulerian velocities are calculated through first- and second-order series expansions. The difference between these two velocities shows the impact of the truncation error in the series expansion. The difference for $St < 0.25$ is shown to be acceptable. In the *a posteriori* test, the results obtained by the first-order equilibrium Eulerian are compared against those obtained by the trajectory approach in which particles are individually tracked in the Lagrangian framework. The mean turbulent kinetic energy, the dissipation rate, and the spectra of the carrier phase are studied in this work. It is observed that the presence of particles with small Stokes numbers significantly changes these statistics in two-way coupling. This observation is in agreement with the recent work by Ferrante and Elghobashi [29]. Moreover, it is shown that the statistics predicated by the equilibrium Eulerian approach are in good agreement with those calculated by the trajectory approach. The deviation between the statistics predicted by these two approaches increases when the particle Stokes number or the mean particle concentration increases. This is basically due to the fact that the increase in the Stokes number results in the decrease in the accuracy of the equilibrium assumption which is made in the development of the equilibrium Eulerian approach [9,10].

[1] M. Ishii, *Thermo-Fluid Dynamic Theory of Two-Phase Flow* (Eyrolles, Paris, 1975).
[2] D. A. Drew, Annu. Rev. Fluid Mech. **15**, 261 (1983).
[3] D. D. Joseph, T. S. Lundgren, R. Jackson, and D. A. Saville, Int. J. Multiphase Flow **16**, 35 (1990).
[4] D. Z. Zhang and A. Prosperetti, J. Fluid Mech. **267**, 185 (1994).
[5] D. Z. Zhang and A. Prosperetti, Int. J. Multiphase Flow **23**, 425 (1997).
[6] O. A. Druzhinin and S. Elghobashi, Phys. Fluids **11**, 602 (1999).
[7] P. Fevrier, O. Simonin, and K. D. Squires, J. Fluid Mech. **533**, 1 (2005).
[8] A. Kaufmann, M. Moreau, O. Simonin, and J. Helie, J. Comput. Phys. **227**, 6448 (2008).
[9] S. L. Rani and S. Balachandar, Int. J. Multiphase Flow **29**, 1793 (2003).
[10] B. Shotorban and S. Balachandar, Phys. Fluids **18**, 065105 (2006).
[11] G. Boffetta, A. Celani, F. De Lillo, and S. Musacchio, Europhys. Lett. **78**, 14001 (2007).
[12] M. R. Maxey, J. Fluid Mech. **174**, 441 (1987).
[13] O. A. Druzhinin, J. Fluid Mech. **297**, 49 (1995).
[14] J. Ferry and S. Balachandar, Int. J. Multiphase Flow **27**, 1199 (2001).
[15] Z. Dodin and T. Elperin, Phys. Fluids **16**, 3231 (2004).
[16] F. Najjar, J. Ferry, A. Haselbacher, and S. Balachandar, J. Spacecr. Rockets **43**, 1258 (2006).
[17] C. Cantero, S. Balachandar, and M. Garcia, Int. J. Multiphase Flow **34**, 484 (2008).
[18] B. Shotorban and S. Balachandar, Phys. Fluids **19**, 118107 (2007).
[19] T. Elperin, N. Kleeorin, and I. Rogachevskii, Phys. Rev. Lett. **76**, 224 (1996).
[20] E. Balkovsky, G. Falkovich, and A. Fouxon, Phys. Rev. Lett. **86**, 2790 (2001).
[21] T. Elperin, N. Kleeorin, V. S. Lvov, I. Rogachevskii, and D. Sokoloff, Phys. Rev. E **66**, 036302 (2002).
[22] G. Falkovich and A. Pumir, Phys. Fluids **16**, L47 (2004).
[23] J. Bec, L. Biferale, G. Boffetta, A. Celani, M. Cencini, A. Lanotte, S. Musacchio, and F. Toschi, J. Fluid Mech. **550**, 349 (2006).
[24] M. R. Maxey and J. J. Riley, Phys. Fluids **26**, 883 (1983).
[25] V. Armenio and V. Fiorotto, Phys. Fluids **13**, 2437 (2001).
[26] J. Ferry, S. L. Rani, and S. Balachandar, Int. J. Multiphase Flow **29**, 869 (2003).
[27] A. M. Ahmed and S. Elghobashi, Phys. Fluids **12**, 2906 (2000).
[28] B. Shotorban, F. Mashayek, and R. V. R. Pandya, Int. J. Multiphase Flow **29**, 1333 (2003).
[29] A. Ferrante and S. Elghobashi, Phys. Fluids **15**, 315 (2003).
[30] F. Mashayek, J. Fluid Mech. **367**, 163 (1998).
[31] F. Mashayek, J. Fluid Mech. **405**, 1 (2000).
[32] V. S. L'vov, G. Ooms, and A. Pomyalov, Phys. Rev. E **67**, 046314 (2003).
[33] R. C. Hogan and J. N. Cuzzi, Phys. Rev. E **75**, 056305 (2007).
[34] K. Luo, J. Fan, and K. Cen, Phys. Rev. E **75**, 046309 (2007).
[35] T. Passot and A. Pouquet, J. Fluid Mech. **181**, 441 (1987).
[36] B. Shotorban, Ph. D. thesis, Universtiy of Illinois at Chicago, Chicago, IL, 2005.
[37] S. B. Pope, *Turbulent Flows* (Cambridge University Press, Cambridge, England, 2000).
[38] J. Bec, L. Biferale, M. Cencini, A. Lanotte, S. Musacchio, and F. Toschi, Phys. Rev. Lett. **98**, 084502 (2007).